

HIGH RESOLUTION X-RAY IMAGING AS A POWERFUL DIAGNOSTICS TOOL TO INVESTIGATE ECRIS PLASMA STRUCTURE AND CONFINEMENT DYNAMICS

E. Naselli^{†1}, D. Mascali, M. Mazzaglia, G. Castro, L. Celona, S. Gammino, G. Torrissi,
INFN-Laboratori Nazionali del Sud, Catania, Italy
R. Rácz, S. Biri, Z. Perduk, J. Pálinkás,
Institute for Nuclear Research (Atomki), Debrecen, Hungary
A. Galatá, INFN-Laboratori Nazionali di Legnaro, Legnaro, Italy
¹also at Name of Università degli Studi di Catania, Catania, Italy

Abstract

High resolution spatially-resolved X-ray spectroscopy, by means of a X-ray pin-hole camera setup operating in the 0.5-20 keV energy domain, is a very powerful method for ECRIS plasma structure evaluation. We present the setup installed at a 14 GHz ECRIS (ATOMKI, Debrecen), including a multi-layered collimator enabling measurements up to several hundreds of watts of RF pumping power and the achieved spatial and energy resolution (0.5 mm and 300 eV). Results coming by a new algorithm for analyzing Integrated (multi-events detection) and Photon-Counted images (single-event detection) to perform energy-resolved investigation will be described. The analysis permits to investigate High-Dynamic-Range (HDR) and spectrally resolved images, to study the effect of the axial and radial confinement (even separately), the plasma radius, the fluxes of deconfined electrons distinguishing fluorescence lines of the materials of the plasma chamber (Ti, Ta) from plasma (Ar) fluorescence lines. This method allows a detailed characterization of warm electrons, important for ionization, and to quantitatively estimate local plasma density and spectral temperature pixel-by-pixel.

INTRODUCTION

Electron cyclotron resonance ion sources (ECRIS) are able to produce beams of highly charged ions with high intensity and stability, which are necessary for accelerators in applied and nuclear physics research. In order to produce these beams, continuous improvement in the performance of ECR ion sources is required and, since the characteristics of the extracted beam (in terms of current intensity and production of high charge states) are directly connected to plasma parameters and structure. Deeper knowledge of plasma properties becomes thus fundamental. Therefore, at INFN-LNS (Istituto Nazionale di Fisica Nucleare – Laboratori Nazionali del Sud) in collaboration with the Atomki laboratories (Debrecen, Hungary), several non invasive diagnostic tools have been developed, with advanced analytical methods. Among the others, an innovative diagnostic tool consisting of a lead pin-hole, a CCD camera and a multi-disks lead collimator is able to perform high spatial and energy resolution imaging and spectroscopy in the soft X-ray domain.

[†] eugenia.naselli@lns.infn.it

It represents a very powerful tool to investigate spectrally resolved images, to study the effect of the axial confinement, the plasma radius evaluation and the fluxes of deconfined electrons, also distinguishing fluorescence lines of each material of the plasma chamber (Titanium, Tantalum) from fluorescence lines of plasma (Argon).

Several experiments have demonstrated that the plasma turbulent regimes cause ECRIS performances deterioration in the extracted ion beam, in terms of beam ripple and a decreasing of the high charge state production [1-3]; even if other works have demonstrated that the plasma stability and the ion beam stability can be improved by applying two frequency heating of the plasma [4-6], further studies are necessary in order to investigate in details this phenomena. Moreover, other works [7] predict that turbulent regimes of plasma can generate *precipitations* of the energetic electrons in the loss cones (producing the X-ray burst emission when they impact in the plasma chamber walls) thus increasing the losses compared to the plasma emission.

In 2014 X-ray space resolved-spectroscopy was already performed, but only in low power regimes up to 30 W of RF pumping power [8, 9]. In order to investigate the turbulent regimes, increasing the pumping RF power at least at about 100 W becomes necessary [10]. On this purpose, the whole diagnostic tool for X-ray imaging has been recently improved. The system was re-designed; a new multi-disks lead collimator able to reduce the noise caused by scattering (that becomes very high in high power domain), an innovative plasma chamber design and analytical methods to post-process the acquired images were introduced. Now 200 W operations are possible (one order of magnitude higher than the previous ones) and the diagnostic system can represent an interesting and powerful method to investigate how the turbulences affects the plasma confinement and losses dynamics.

EXPERIMENTAL SETUP

The measurement was carried out in the 2th generation ECRIS installed in the ECR Laboratory of ATOMKI, in Debrecen (Hungary) [11]. The basic operation frequency is 14.25 GHz provided by a klystron amplifier, but it is also possible heating the plasma with a second (tuneable) frequency provided by a travelling wave tube (TWT) amplifier. The axial magnetic field is 1.26 T (injection),

0.39 T (B_{\min}) and 0.92 T (extraction), whilst the radial magnetic field produced by a permanent magnet hexapole and measured at the plasma chamber wall ($R=29$ mm) is 1.1 T. The length of the plasma chamber is 210 mm and the diameter 58 mm.

The non-invasive diagnostic tool consists of:

- a CCD camera, with a sensitive range 2 keV – 20 keV, made of 1024x1024 pixels and having a sensor size 13.3 x 13.3 mm;
- a lead pin-hole of 2 mm of thickness and 400 μm of hole diameter, which is able to reproduce the plasma image in the CCD position-sensitive detector. The magnification M of the pin-hole system (developed by the position of the pin-hole with respect to the plasma and to the CCD chip) was optimized: $M=0.24$;
- two Titanium windows with a total thickness of 9.5 μm in order to reduce UV and visible light;
- a multi-disks collimator consisting of two lead disks of 1 mm of thickness was installed at 40 mm from the pin-hole on the CCD side and 6 mm on the plasma side. The hole diameters are 1 mm and 2 mm, respectively.

A sketch of the whole system is shown in the Fig 1.

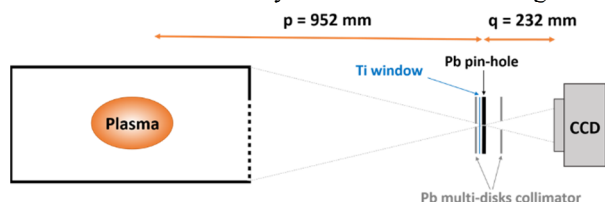


Figure 1. Sketch of the X-ray pin-hole camera setup.

Moreover, a special design of the plasma chamber walls covered by a liner of Tantalum (for the lateral walls) and Titanium and Aluminum (for the extraction and injection endplate, respectively) has been implemented in order to distinguish between fluxes of X-rays coming from walls' bremsstrahlung and fluorescence (produced by the electrons escaping the magnetic trap and impinging on the metals surfaces), from the ones coming from the Argon plasma (due mainly to the fluorescence of the confined ions).

Multi-collimator to Investigate High Power Regimes

By developing the multi-disks lead collimator as extra shielding it has been possible to acquire X-ray picture in relatively high RF-power operation mode, up to 200 W total incident power. This datum still represents the highest operative RF power for which X-ray imaging has been never performed in the field of ECR Ion Sources and ECR compact traps.

Figure 2 shows the two images acquired in the same operative configuration (pumping RF power of 200 W and RF frequency of 13.9 GHz) with an exposure time of 50 seconds have been reported: the image 2.a) has been acquired without the usage of the collimator, the 2.b) with it. It has been demonstrated that using the collimator the noise decrease of 405% outside the plasma chamber (considering

the total counts in the region of interest (ROI) squared in green, in the images) and of 152% inside the plasma chamber (considering the total counts in the ROI squared in cyan, in the images). Whilst the signal/noise ratio increase of 70% and 39% outside and inside the plasma chamber, respectively. The signal has been estimated considering the total counts in the ROI white squared.

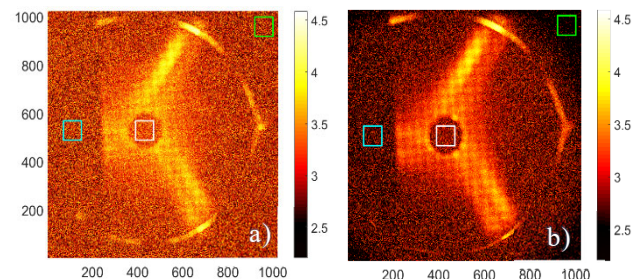


Figure 2. Pseudo-color elaboration of X-ray flux (in logarithmic scale), putting in evidence the ROI where the radiation coming from Ar plasma only (squared in white), and the ROIs where radiation is due to scattering effects (squared in cyan and in green). a) - without the multi-disks collimator. b) - in the pin-hole setup the multi-disks collimator has been used.

Moreover, a very high spatial resolution (500 μm [12]) can be obtained by using the collimator; in the Fig. 2.b) it is in fact possible well distinguish the mesh structure of the Aluminum endplate, manufactured in order to shield microwave but guarantee above 60% of X-ray transmission. The wire diameter is only 400 μm .

THE X-RAY IMAGE OPERATIVE MODES

The photon impinging in the camera generates charge that is proportional to the deposited energy. The Analogue Digital Unit (ADU), corresponding to every pixels and finally read by the CCD, is proportional with the product of the incident photons and their energies. Typically, there are two main operative modes to acquire the images: the *Spectrally Integrated (Spl)* mode and the *Single Photon Counting (SPhC)* mode.

During a long exposure time - for example images collected with several tens of seconds - multi events are registered by the CCD camera, and the spectral information of the incoming X-rays is lost. Therefore, images obtained with long exposure times are called *Spectrally Integrated images*. In this case energy separation of the events is not possible, however, ADUs are revealing the energy content of the plasma and plasma chamber complex. The advantage, in this case, is that these acquisitions are typically fast (tens of seconds) and it is so possible to master, likely "on line", the changes of plasma structure and morphology.

The more powerful investigations, able to perform local energy determination, is provided by *Single Photon Counting* mode. Decoupling of photon number versus energy is possible. The technique allows to perform space-resolved spectroscopy (thus evidencing the local displacement of electrons at different energies, as well as of plasma ions highlighted by fluorescence lines emission) versus the

main tuning parameters such as the pumping wave frequency and the strength of the confining magnetic field. It is very useful in order to study how the operative parameters (RF pumping frequency and power, magnetic field and also phenomena such as plasma turbulence) affect the plasma confinement, stability and turbulence onset and to investigate dynamics of plasma versus plasma losses.

The SPhC mode is obtained by fixing a short exposure-time for each of the acquired image-frame (typically in the range of several tens of milliseconds). Multi-images are recorded in SPhC (of the order of thousands image-frames). The SPhC mode allows minimizing the probability that two (or more) photons hit the same pixel during the exposure of a single image-frame with a consequent loss of information about their energies. Only a few number of pixels is illuminated on the full CCD matrix and they can be associated with single photon events and, consequently, they carry the information (in terms of charge) on the energies of the incident photons.

Development of a proper acquisition and processing procedure of the experimental data were required and advanced analytical methods were needed and have been developed on purpose.

THE ANALYTICAL METHOD

Analytical algorithm has been developed to elaborate the raw data acquired using the X-ray pin-hole camera tool, in particular to analyze the Single Photon-Counting images, to perform energy-resolved investigation pixel-by-pixel and deep investigations about confinement dynamics. The analytical method has been developed using the MatLab programming platform.

The developed analytical method for SPhC imaging and spectroscopy consists of six different steps. In this section we describe only the main step, the so called *Grouping process (Gr-p)*, that allows performing the space-resolved spectrum.

Even working in SPhC mode, multipixel events are always present in each of the image-frames acquired during the measurement: they could be associated with a *single photon* that interacts with more than one pixel, or *two (or more) photons* that hit neighboring pixels. The algorithm has been elaborated for recognizing and correcting the group-events.

To ensure the incoming photon energy proportional to the sum of ADU of the loaded pixels, it is necessary that in each acquired image-frame one photon only releases its energy in a given group of pixels. Whilst, if photons are fall to two pixels close to each other, the pixels loaded by the two photons are overlapped or become neighbours forming large clusters and the energy of the photons are summed in this big cluster. Since the isolation of the effect of the two or more photons contributions are impossible, these spurious events have to be filter out by the analytical algorithm. On this purpose, we introduced an input parameter in the algorithm, called *S parameter*, that represents the maximum cluster *size* (*size* is defined as the number of neighbours pixels compounding a cluster) that can be considered due to the impact of only one photon. Consequently, all the

clusters of pixels having size larger than S have been filtered out by the algorithm. Moreover, also the offset noise contribution has been removed setting a threshold called *L value*.

In a nutshell, the two main input parameters used to characterize the script-run are:

- L = count Limit, the threshold to consider a pixel as cluster component, this limit set a noise level;
- S = cluster Size, the maximum number of connected pixels to consider them as not overlapping counts.

In more detail, the algorithm works in the following mode: considering a given image-frame, the first phase consists in "*turning off*" all pixels having ADU lower than L , putting to zero all their values; later the procedure scans pixel by pixel each of the image and when an illuminated pixel of coordinates (X, Y) is identified, its neighbouring pixels are checked. If no charge is present into the surrounding pixels, the event is considered to be generated by a single photon and it is associated with a 3-coordinates point (X, Y, E) . The coordinate E is the energy associated with the photon. When a group of neighboring pixels is identified during the scan of an image-frame, the algorithm processes this multipixel event to reconstruct its nature (i.e., single or multiple-hit):

- in the group associated with a single photon-event (typically characterized by the presence of a pixel with a maximum intensity, in terms of charge) the code perform the integration of the total charge giving the energy of the photon; the hitting coordinate (X, Y) is fixed to the pixel containing the maximum contribution;
- in case of the groups associated with multiple-hit events (typically characterized by the presence of different relative maxima in a large size of the group of pixels) the processing algorithm filter out them.

When the pixel in the position (X,Y) has been elaborated, the algorithm start to process the subsequent pixel in the position $(X+1,Y)$. The above procedure is repeated pixel by pixel in all the frames.

Considering, for example, a ROI (Region of Interest) of the pixelated matrix (1024x1024 pixels) correspondent to an image-frame, it is possible to observe how the different steps of the Gr-p elaborates the images: we can consider a setting $S=5$ and $L=10$ as input parameters in the algorithm.

A ROI of 20X30 pixels, by way of example, has been considered in the Fig. 3. The image shown in Fig. 3 a) is corresponding to the first phase, where all pixels having charge lower than L (putted to zero). Moreover, in this step, the algorithm finds and checks the clusters size (in red squared the clusters having size larger than S , in green squared the other ones). As it is possible to observe, the first ones typically present two or more local maximum, highlighting the contribution does not due by one only single photon. On this purpose, the second step filters out them (the image with the ADU values is shown in Fig. 3. b).

Finally, the third step integrates the charge of all pixels composing a given cluster shown in Fig. 3. c).

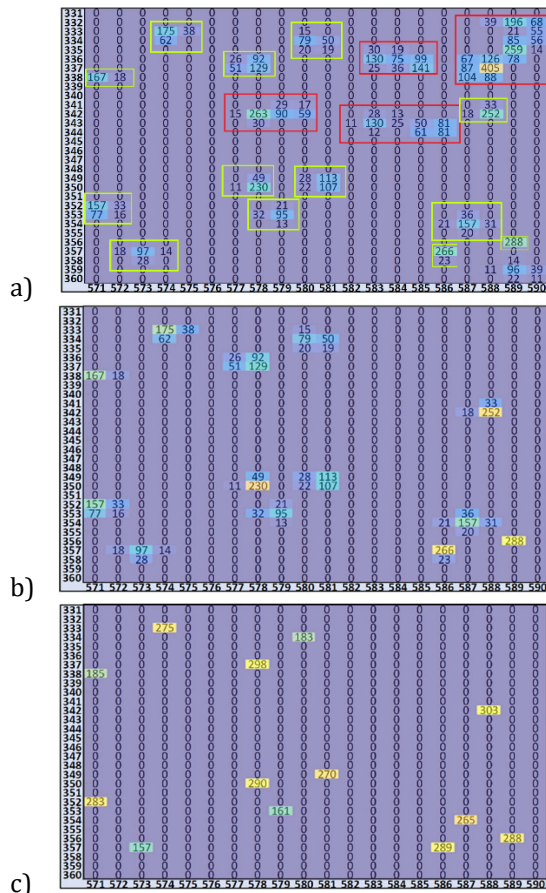


Figure 3: ROI of 20X30 pixels elaborated implementing the three different steps of the grouping procedure: a) after the first step; b) after the second step; c) after the third step.

After that the Gr-p has been performed for all the image-frames composing a measurement, it is assigned a variable N to each coordinate (X, Y) of the CCD matrix; N is the number of photons with energy E in the position (X, Y) . N is incremented by a unit during the scansion of all the frames when a photon of energy E is detected in the same position (X, Y) in another frame K .

At the end of the scansion of all the image-frames a set of points with coordinates (X, Y, E, N_{tot}) is obtained. The plot of the total counts N_{tot} versus the energy E is the full X-ray spectrum of the sample under investigation.

THE EXPERIMENTAL RESULTS

In this section an overview of the experimental results concerning both the integrated imaging and the space-resolved spectroscopy in SPHC will be presented.

The Integrated X-ray Imaging

The *Integrated X-ray Imaging* consists in acquiring only one image with a long exposure time of the order of tens of seconds. In this case the total measurement time results to be very fast and the elaboration of the image needs an easy analysis.

An example of a power scaling of the integrated images is shown in Fig. 4 (RF frequency = 13.8 GHz) varying the pumping RF power from 20 W to 200 W at step of 20 W.

From a visual inspection it is possible to highlight how the energy content changes vs. the pumping power.

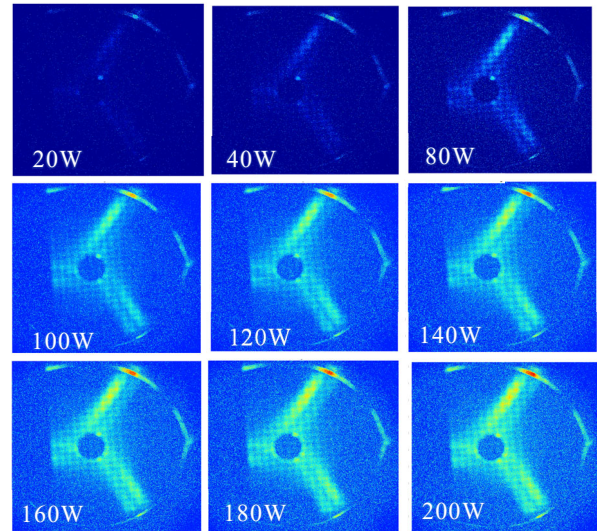


Figure 4: Pseudo-color elaboration of X-ray images (in the same logarithmic scale): power scaling, from 20 W up to 200 W.

Selecting specific ROIs in the images it is also possible to quantitative investigate about the energy content of the emission, comparing the plasma emission vs. the losses emission. It has demonstrated that in the stable regimes the losses decrease [5] and the plasma is rearranged to be denser in a central region of the plasma [13].

Moreover, with integrated imaging it is also possible to *on-line* measure the plasma radius: i.e., at 13.9 GHz of pumping frequency, the experimental radius results 16.04 ± 1.44 mm, which is in very good agreement with the radius of the ECR-ellipsoid (15.50 mm) estimated using the realistic magnetic field of the Atomki-ECRIS.

PhC Imaging and Space-Resolved Spectroscopy

Figure 5 shows the reports of the full field X-ray spectrum of an acquired configuration, with a total net RF pumping power of 200 Watt and a FR frequency of 13.9 GHz amplified by the TWT.

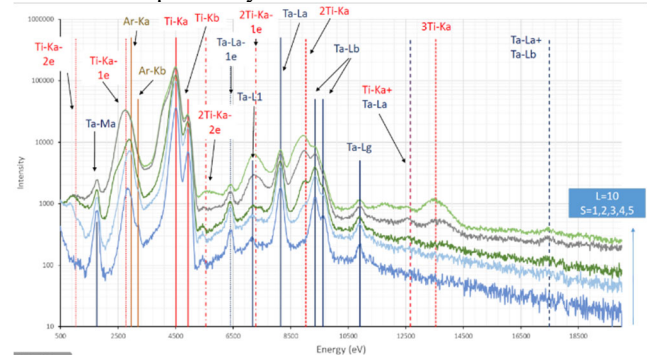


Figure 5: Full field X-ray spectrum of experimental configuration acquired with a total net RF pumping power of 200 Watt and a FR frequency of 13.9 GHz amplified by the TWT.

The thousands of image-frames are gaining the statistics necessary for elaborating high quality X-ray fluorescence spectra and images.

It is possible to distinguish fluorescence lines of each material of the plasma chamber (Ti, Ta) and the fluorescence lines of plasma (Ar). There are also dimer peaks and escape peaks for each fluorescence line. The energy resolution is 0.326 keV at 8.1 keV [12], corresponding to the Ta-L α line. Separated characteristic peaks in the X-ray spectra, coming from each material, allow to study the confinement dynamics (plasma vs losses X-ray emission) discriminating the radial losses from the axial losses also: X-rays coming from magnetic branches (where electrons are axially deconfined) consist of mostly fluorescence from Ti, X-rays coming from plasma are mostly due to ionized K α Argon lines and X-rays coming from poles (where electrons are radially deconfined) are mostly due to radial losses impinging on the Ta liner.

Moreover, since the data on the spectrum contains the spatial information on the emitting positions, the definition of a ROI on the fluorescence peaks in the spectrum allows the imaging of the elemental distribution, and it is possible to distinguish the emission (and the correspondent image) coming from each material. As it is possible to highlight in Fig. 6, it is possible to distinguish the emission coming from Ar plasma only (selecting the fluorescence from Ar only), compared to the radial losses (Ta) or the axial losses (Ti), selecting the fluorescence from Titanium and Tantalum, respectively.

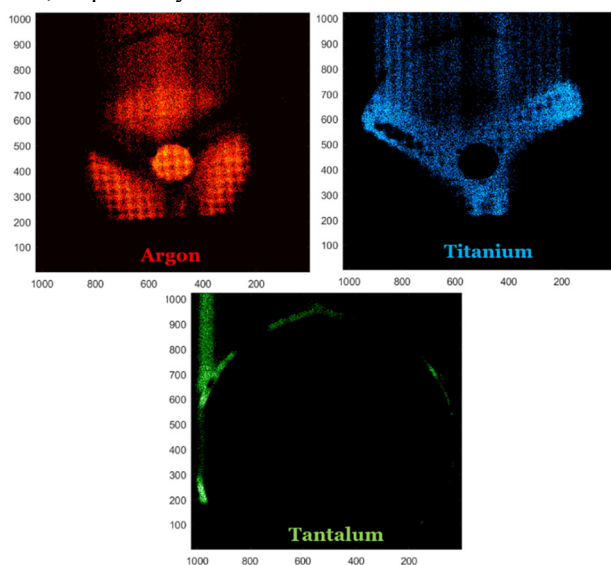


Figure 6: 2D energy filtered images showing fluorescence photons coming from the argon plasma and signals coming from the metallic layers covering plasma chamber walls.

Finally, it is possible also perform a complementary analysis: selecting in the whole image only a “collection” of pixels of a ROI, it is possible to investigate about the elemental composition in the given ROI only by means of the correspondent spectrum and, consequently, to perform the plasma parameters (electron density and temperature) estimation.

CONCLUSION AND PERSPECTIVES

The paper reports the tool, the analytical method and the preliminary results of a powerful system for making plasma physics investigation by means of spectrally-resolved imaging and space-resolved spectroscopy. *Live* plasma structure and emission investigations can be performed, using Integrated imaging, and correlating the results vs. ECRIS operative parameters.

The more powerful analysis consists in the Spatial-Resolved Spectroscopy for quantitative estimation of deconfined fluxes in stable vs. unstable regimes, quantitative elemental composition determination pixel-by-pixel and locally plasma parameters (electron density, temperature) measurements.

In perspectives, space-resolved soft X-ray analysis will investigate how plasma turbulence and plasma heating method (i.e. the Two-Close-Frequency Heating) affect plasma confinement and loss dynamics.

ACKNOWLEDGMENTS

The authors gratefully acknowledge the support of INFN by the Grants PANDORA (5th Nat. Comm.) and PANDORA_GR3 (3rd Nat. Comm.).

REFERENCES

- [1] S. Gammino, D. Mascali, L. Celona, F. Maimone and G. Ciavola, “Consideration on the role of the magnetic field gradient in ECR ion sources and build-up of hot electron component”, *Plasma Sources Science and Technology*, vol. 18, issue no. 4, p. 045016, 2009.
doi.org/10.1088/0963-0252/18/4/045016
- [2] O. Tarvainen, J. Laulainen, J. Komppula, R. Kronholm, T. Kalvas, H. Koivisto and V. Skalyga, “Limitations of electron cyclotron resonance ion source performances set by kinetic plasma instabilities”, *Rev. of Sci. Instrum.*, vol. 86, p. 023301, 2015.
doi.org/10.1063/1.4906804
- [3] A. Kitagawa *et al.*, “Two-frequency Heating Technique for Stable ECR Plasma”, in *Proc. 20th Int. Workshop on ECR Ion Sources (ECRIS'12)*, Sydney, Australia, Sep. 2012, paper TUXO03, pp. 10-12.
- [4] V. Skalyga, I. Izotov, T. Kalvas, H. Koivisto, J. Komppula, R. Kronholm, J. Laulainen, D. Mansfeld and O. Tarvainen, “Suppression of cyclotron instability in Electron Cyclotron Resonance ion sources by two-frequency heating”, *Physics of Plasmas*, vol. 22, p. 083509, 2015.
doi.org/10.1063/1.4928428
- [5] E. Naselli, D. Mascali, M. Mazzaglia, S. Biri, R. Rácz, J. Pálkás, Z. Perduk, A. Galatá, G. Castro, L. Celona, S. Gammino and G. Torrissi, “Impact of two-close-frequency heating on ECR ion source plasma radio emission and stability”, *Plasma Sources Sci. Technol.*, vol. 28, p. 085021, 2019.
doi.org/10.1088/1361-6595/ab32f9
- [6] R. Racz *et al.*, “Effect of the Two-Close-Frequency Heating to the extracted ion beam and to the X-ray flux emitted by the ECR plasma”, *JINST*, vol. 13, p. C12012, 2018.
doi.org/10.1088/1748-0221/13/12/C12012

- [7] A. G. Shalashov *et al.*, “Kinetic instabilities in a mirror-confined plasma sustained by high-power microwave radiation” *Phys. Plasmas*, vol. 24, p. 032111, 2017.
doi.org/10.1063/1.4978565
- [8] R. Rácz, D. Mascali, S. Biri, C. Caliri, G. Castro, A. Galatà, S. Gammino, L. Neri, J. Pálinkás, F. P. Romano and G. Torrisi, “Electron cyclotron resonance ion source plasma characterization by energy dispersive x-ray imaging”, *Plasma Sources Sci. Technol.*, vol. 26, p. 075011, 2017.
doi.org/10.1088%2F1361-6595%2Faa758f
- [9] D. Mascali *et al.*, “Electron cyclotron resonance ion source plasma characterization by X-ray spectroscopy and X-ray imaging”, *Rev. Sci. Instrum.*, vol. 87, p. 02A510, 2016.
doi.org/10.1063/1.4939201
- [10] A. G. Shalashov *et al.*, “Kinetic instabilities in a mirror-confined plasma sustained by high-power microwave radiation”, *Physics of Plasmas*, vol. 24, p. 032111, 2017.
doi.org/10.1063/1.4978565
- [11] S. Biri, R. Rácz and J. Pálinkás, “Status and special features of the Atomki ECR ion source”, *Rev. Sci. Instrum.*, vol. 83 p. 02A341, 2012.
doi.org/10.1063/1.3673006
- [12] E. Naselli *et al.*, “Multidiagnostics setups for magnetoplasmas devoted to astrophysics and nuclear astrophysics research in compact traps”, *JINST*, vol. 14, issue no 10, 2019.
doi.org/10.1088/1748-0221/14/10/C10008
- [13] R. Racz *et al.*, “Imaging in X-ray ranges to locally investigate the effect of the Two-Close-Frequency Heating in ECRIS plasmas”, presented at the 24th International Workshop on ECR Ion Sources (ECRIS’20), paper MOYZO01, this conference.